Soft Matter

RSC Publishing

PAPER

Osmotic propulsion of colloidal particles *via* constant surface flux

Cite this: *Soft Matter*, 2013, **9**, 6382

U. M. Córdova-Figueroa,*[a] J. F. Brady*[bc] and S. Shklyaev[abd]

We propose a model for the self-propulsion of a small motor particle that generates a nonuniform concentration distribution of solute in the surrounding fluid *via* a constant solute flux asymmetrically from the motor surface. The net osmotic driving force and motor speed are investigated in the limits of slow and fast product particle flux (relative to the diffusive flux of the product species). When the only solute species in solution is that produced by the motor, the motor's speed is shown to be proportional to the solute flux for slow flux rates and to the square root of the solute flux for large flux rates. When solute species are already present in solution at concentration high compared to that generated by the motor, the motor speed at high flux rates saturates and scales as the diffusivity of the solute divided by the motor size. The analytical results compare well with Brownian dynamics simulations. Full hydrodynamic interactions are taken into account in the theoretical analysis.

Received 2nd January 2013
Accepted 22nd May 2013

DOI: 10.1039/c3sm00017f

www.rsc.org/softmatter

1 Introduction

Achieving autonomous motion or self-propulsion of colloidal-scale objects in a fluid medium is an important challenge in materials science and engineering. Currently, much of the experimental effort relies on the synthesis of colloidal devices from a variety of building blocks that induce work or motion from 'on-board' power sources—without the need of external forces or inputs.[1] As envisioned by Ozin *et al.*,[2] these devices, whether individual or assembled into desired architectures, might someday transport medicine in the human body, conduct operations in cells, move cargo around microfluidic chips or complex channels, manage light beams, agitate liquids close to surfaces, and search for and destroy toxic organic molecules in polluted water streams.

In the past decades, researchers have investigated a variety of external fields for colloidal transport in fluids, such as electrophoresis for directing charged particles by an electric field,[3] thermo- and diffusiophoretic migration due to temperature and solute concentration gradients,[4,5] respectively, and optical tweezers to manipulate particles using intense light gradients.[6] However, as shown in several experiments, phoresis of particles can not only be induced externally, but also by on-board processes, such as catalytic reactions[7,8] and heat generation[9] that change the physical properties of the particle's environment and thus create local gradients. Similar manifestations, but at smaller length scales, are found in many physicochemical processes in biology where chemical gradients drive the dynamics of many components of a cell. For example, polymerizing networks of actin filaments generate motion in a variety of living cells, *e.g.* intra- and inter-cellular motility of certain bacterial and viral pathogens, and motility of endocytic vesicles and other membrane-bound organelles. Moving intracellular bacteria display phase-dense 'comet tails' made of actin filaments, the formation of which is required for motility.[10]

Theoretical work on the self-propulsion of nonliving, catalytic particles was initiated by Golestanian *et al.*,[11,12] who used the classical continuum approach to diffusiophoretic motion,[5] replacing the imposed concentration gradient by a locally generated one. Various distributions of a chemical reaction over the surface of a self-propelling particle (either a sphere or a rod) can give rise to net propulsion, and the simplest model of a prescribed flux of chemical species at the motor surface was used by these authors. They considered the limit of slow motor motion so that the solute only diffuses in the surrounding fluid. Subsequent experiments by Howse *et al.*[8] agreed with some predictions from the theory for a half-reactive, or Janus, spherical motor.

Córdova-Figueroa and Brady[13] also studied the self-propulsion of catalytic particles but adopted a colloidal description in which both the motor and the chemical solute species are modeled as colloidal particles dispersed in an incompressible fluid or solvent. They showed that the motion of the motor particle could be understood in terms of a balance between the Stokes drag on the motor and the net 'osmotic' force exerted by the solute particles owing to the nonequilibrium distribution of solute caused by a surface chemical reaction on the motor.

[a]*Department of Chemical Engineering, University of Puerto Rico – Mayagüez, Mayagüez, PR 00681, USA. E-mail: ubaldom.cordova@upr.edu*

[b]*Division of Chemistry & Chemical Engineering, California Institute of Technology, Pasadena, CA 91125, USA. E-mail: jf brady@caltech.edu*

[c]*Division of Engineering & Applied Science, California Institute of Technology, Pasadena, CA 91125, USA*

[d]*Institute of Continuous Media Mechanics, Ural Branch of Russian Academy of Sciences, Perm, 614013 Russia*

The work of Córdova-Figueroa and Brady[13] was questioned by Jülicher and Prost[14] who believe that an osmotic pressure or force cannot give rise to self-propulsion. However, as shown in detail by Brady,[15] Jülicher and Prost[14] did not appreciate that Córdova-Figueroa and Brady[13] were modeling the process at a more fundamental colloidal level than the customary continuum description, and at this level osmotic forces are operative (see Fig. 1). Indeed, Brady[15] showed that this colloidal approach reproduces the conventional treatment of diffusiophoresis[5] and showed how to incorporate hydrodynamic interactions (HI) into the work of Córdova-Figueroa and Brady.[13]

Another feature of the colloidal description is the ability to incorporate the finite size ratio and various interaction potentials between the motor and the solute species, and thereby address, for example, the self-propulsion of a gene or a large protein complex in response to chemical reactions. Recently, Sharifi-Mood *et al.*[16] have re-examined self-diffusiophoresis from the continuum perspective, explicitly allowing for surface chemical reaction and various interaction potentials, and have derived results in complete agreement with the colloidal description of Brady.[15]

In contrast to the prescribed flux study of Golestanian *et al.*,[11,12] Córdova-Figueroa and Brady[13] addressed the problem of a first-order chemical reaction on a Janus motor particle (an osmotic motor) and considered the limits of fast and slow chemical reactions and explicitly included the advective motion of the motor on the concentration distribution of reactants/products in the surrounding fluid. This advective motion leads to a maximum in the motor speed given by the diffusive velocity of the reactants/products—the reactant/product diffusivity divided by the motor size.

In this article we follow the colloidal approach of Córdova-Figueroa and Brady[13] and Brady[15] and examine the motion of an osmotic motor with a prescribed asymmetric surface flux, j_s, of a product species. It is shown that when the solution is initially free of solute and at small flux rates, in agreement with the continuum analysis of Golestanian *et al.*,[11,12] the motor speed is given by $U = j_s kT\delta^2/8\eta D_b$, where D_b is the diffusivity of the product species, kT is the thermal energy, η is the viscosity of the solvent and δ is the length scale characterizing the interaction between the motor and the product species, which is presumed to be much smaller than the motor size a (the thin interfacial limit). As is customary in phoretic problems, the speed is independent of the motor size a.

At the other extreme of high flux rates, the advection of the motor dominates and sets the distribution of the product solute resulting in a nonanalytic dependence of the motor speed on the solute flux: $U = \sqrt{j_s\, akT/3\eta}$; the motor speed is independent of the interactive length δ and now depends on the motor size. Thus, large motor velocities may be possible at high flux rates. This square root scaling at high flux rates differs from that predicted by Jülicher and Prost;[14] this difference is explained in Section 2.2.

When product species are already present in solution, they hinder the motion of the motor particle by increasing the effective viscosity of the solution, akin to the hindering effect observed in the microrheology of colloidal dispersions.[17–19] When the ratio of the concentration of the already present product species, n^p_∞, to the rate of production of additional products is large, $n^p_\infty D_b/j_s a \gg 1$, the hindering effect dominates and the motor speed is limited by the diffusive velocity of the products, $U \sim D_b/a \times 1\Big/\sqrt{n^p_\infty D_b/j_s a} = \sqrt{j_s D_b/n^p_\infty a}$.

The paper is organized as follows: In Section 2 the problem is formulated and solved for the simplest case when the solvent is free of additional product particles. The additional hindrance resulting from the background concentration of the solute particles is studied in Section 3. Conclusions are given in Section 4.

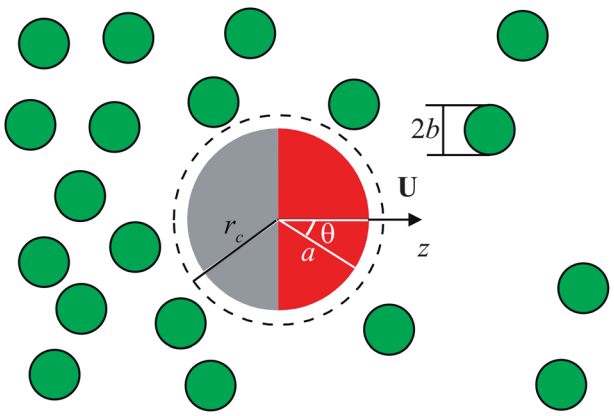

Fig. 1 Schematic description of the constant flux osmotic motor of radius a. The left half of the motor produces a constant flux, j_s, of solute particles of radii b. A net osmotic force on the motor is generated by the nonuniform solute distribution leading to a motor velocity $\boldsymbol{U}$ towards lower solute particle concentration. The solute-motor interactive length $\delta = r_c - a$ is shown as the dashed circle. Solute particles are excluded from the region δ near the motor surface but the solvent is not; the dashed circle thus represents the semipermeable membrane for the osmotic pressure.

2 Motor motion in a solute-free fluid

We consider a particle of radius a that releases product particles of radii b on a portion of its surface as illustrated in Fig. 1. This release could be by a surface catalytic reaction, by the particle ejecting solute or the particle could simply be dissolving into the surrounding fluid. Both the motor and the solute particles are taken to be large compared to the background solvent molecules so that their behavior can be described by the familiar equations of colloidal dynamics.[20] One may not be accustomed to associating a size with the solute, rather characterizing the solute by its diffusivity D_b; the two are equivalent *via* the Stokes–Einstein–Sutherland relation $D_b = kT/6\pi\eta b$, where kT is the thermal energy and η is the viscosity of the suspending fluid. For many situations and the case we shall consider in this work, $b \ll a$, and thus the limit discussed by Brady[15] is appropriate in which the solute has no size and is dilute $\phi_s = 4\pi b^3 n/3 \ll 1$, where n is the number density of solute particles (units of number/volume). In this small b/a limit hydrodynamic interactions between the motor and the solute simplify considerably.[15] To treat the more general case in which

the solute is not small compared to the motor nor at infinite dilution, *i.e.* beyond the leading $O(\phi_s)$ behavior, the reader is referred to the general treatment given by Brady.[15]

To make the analysis as simple as possible we keep the orientation of the motor fixed, neglecting the reorienting effects of Brownian rotations. The time to establish the steady concentration distribution of solute about the motor scales as a^2/D_b, while the time for rotation of the motor is given by inverse of its rotary diffusivity $1/D_R \sim 8\pi\eta a^3/kT$; their ratio is $O(b/a \ll 1)$ showing that the solute distribution researches a steady state before the motor reorients by Brownian rotation. Owing to the Brownian rotation, however, the long-time displacement of the motor will ultimately be diffusive.[8,21]

We model the non-hydrodynamic interaction between the solute and the motor as a hard-sphere-like potential—the solute is excluded from being any closer to the motor than a length δ. This choice avoids the need to know anything precise about the solute-motor interactions—a single parameter, δ, characterizes them, rather than both a length and an amplitude as would be necessary with a soft potential. Further, no potential enters into the equation for the distribution of solute about the motor; the flux condition now appears at the contact radius $r_c = a + \delta$, rather than at the actual motor surface $r = a$ if a continuous potential were used. (The case of a general potential is discussed in detail by Brady.[15]) Note that although the solute is excluded from being any closer to the motor than the length δ, the solvent is not (see Fig. 1). Thus, the interactive length δ acts as the semipermeable membrane customary in osmotic processes.

Under these conditions, Brady[15] showed that the velocity of the motor is given by the following simple formula (see eqn (2.7) of the cited paper)

$$\boldsymbol{U} = U\boldsymbol{e}_z = -\frac{L(r_c)}{6\pi\,\eta a}\oint_{r_c} \boldsymbol{n}\Pi(\boldsymbol{r})\,\mathrm{d}S, \tag{1}$$

where $L(r_c)$ is a nondimensional hydrodynamic function (see below) evaluated at the contact radius r_c, $\boldsymbol{n}$ is the outer normal to the motor surface, $\mathrm{d}S$ is the element of this surface area, the z-axis is the direction of particle motion with unit vector $\boldsymbol{e}_z$ and $\Pi(\boldsymbol{r}) = n(\boldsymbol{r})kT$ is the local osmotic pressure of the solute with number density $n(\boldsymbol{r})$. Eqn (1) affords the straightforward interpretation: the motor velocity is the product of a hydrodynamic mobility, $L(r_c)/6\pi\eta a$, times the net osmotic force exerted on the motor by the solute, $\oint_{r_c}\boldsymbol{n}\Pi(\boldsymbol{r})\mathrm{d}S$.

The solute diffuses and is advected in the fluid with flux relative to the motor $\boldsymbol{j} = -D_b\nabla n + \boldsymbol{u}n$. At the contact surface of the motor, $r = r_c$, the flux boundary condition is $\boldsymbol{n}\cdot\boldsymbol{j} = j_s h(\boldsymbol{n})$, where j_s is the (constant) surface flux of solute from the motor into the surrounding fluid (with units of number/area-time) and $h(\boldsymbol{n})$ is a nondimensional function that specifies the asymmetric distribution of solute flux from the motor surface. An appropriate scale for the concentration is thus $n_s = j_s r_c/D_b$, and we define a nondimensional concentration $\hat{n} = n/n_s = n/(j_s r_c/D_b)$. The nondimensional concentration satisfies the following boundary value problem (see eqn (5.9) of Brady[15] appropriately modified for a specified flux as opposed to a first-order chemical reaction)

$$\nabla^2\hat{n} + \mathrm{Pe}\boldsymbol{e}_z\cdot(L(r)\hat{\boldsymbol{r}}\hat{\boldsymbol{r}} + M(r)(\boldsymbol{I} - \hat{\boldsymbol{r}}\hat{\boldsymbol{r}}))\cdot\nabla\hat{n} = 0, \tag{2a}$$

$$\boldsymbol{n}\cdot\nabla\hat{n} + \mathrm{Pe}\boldsymbol{e}_z\cdot\boldsymbol{n}L(1)\hat{n} = -h(\boldsymbol{n}) \text{ at } r = 1, \tag{2b}$$

$$\hat{n} \to 0 \text{ as } r \to \infty, \tag{2c}$$

where $\hat{\boldsymbol{r}} = \boldsymbol{r}/r$. All lengths have been scaled with the contact radius r_c.

We shall take the asymmetric distribution function to be axisymmetric about the direction of motion $h(\boldsymbol{n}) = h(\theta)$, where $\boldsymbol{e}_z\cdot\boldsymbol{n} = \cos\theta = \mu$. We take $h = 1$ for $\theta > \alpha$ and $h = 0$ otherwise. In the analysis below, we set $\alpha = \pi/2$, unless otherwise stated. In writing eqn (2) we have neglected the diffusion of the motor, which has a Stokes–Einstein–Sutherland diffusivity $D_a = kT/6\pi\eta a$, as compared with that of the solute.

The distribution of the solute concentration depends on the Péclet number $\mathrm{Pe} = Ur_c/D_b$, measuring the relative importance of advection of the solute to diffusion, which, from eqn (1), is given by

$$\mathrm{Pe} = \frac{Ur_c}{D_b} = -\frac{3}{2}\beta_e\,L(1)\int_{-1}^{1}\hat{n}(r=1,\mu)\mu\mathrm{d}\,\mu, \tag{3}$$

where we have defined the nondimensional volume fraction of solute

$$\beta_e \equiv \frac{4\pi}{3}n_s\,{r_c}^3\left(\frac{b}{a}\right) \equiv \frac{4\pi}{3}\frac{j_s\,{r_c}^4}{D_b}\frac{D_a}{D_b}, \tag{4}$$

which is equivalent to a nondimensional flux of solute from the motor. The nondimensional flux β_e is the product of the small solute volume fraction $\phi_s = (4\pi/3)b^3n_s$ and the large geometric factor ${r_c}^3/b^2a$, and thus can take on all values.

The constant flux motor differs from the case considered by Córdova-Figueroa and Brady[13] where the flux at the motor surface was given by a first-order chemical reaction $\boldsymbol{n}\cdot\boldsymbol{j} = -\kappa n h(\boldsymbol{n})$, rather than a constant value $\boldsymbol{n}\cdot\boldsymbol{j} = j_s h(\boldsymbol{n})$. In the reaction rate problem there is a natural limit to the speed of the motor set by how fast the reactant (or solute) can diffuse, D_b/r_c; the concentration at the motor surface cannot decrease below zero as the Damkhöler number, $Da = \kappa r_c/D_b$, is increased. For a constant flux motor there is no diffusion limiting process and, as we shall see, the motor velocity can become quite large for large flux rates (large β_e).

A second important dimensionless parameter, $R_c = r_c/a = 1 + \delta/a$, enters *via* the hydrodynamic mobility functions:[15,22]

$$L(r) = 1 - \frac{3}{2rR_c} + \frac{1}{2\,(rR_c)^3};\; M\,(r) = 1 - \frac{3}{4rR_c} - \frac{1}{4\,(rR_c)^3}. \tag{5}$$

It is clear that for $R_c \gg 1$ no hydrodynamic interactions (HI) enter as $L = M = 1$, while in the opposite case $R_c = 1$ the lubrication forces prevent the solute particles from touching the motor and exerting a force on it. In this case one needs the more complete analysis by Brady[15] which shows that the speed is proportional to the ratio of the solute to motor size squared, (b/a).[2] In this work we shall take the interactive potential length $\delta > b$ so that the near-field lubrication forces are not important and so that we may make contact with the conventional continuum treatment of such phoretic-like processes. Varying the parameter R_c thus allows us to systematically vary HI.

2.1 Small flux rates, $\beta_e \ll 1$

At small β_e the Péclet number is small and advection is weak and the terms proportional to Pe can be omitted in eqn (2). The resulting diffusion equation can be solved analytically by separation of variables with solution in terms of decaying harmonics. The Péclet number is then found from eqn (3) as

$$\mathrm{Pe} = \frac{3}{8}\beta_e L(1), \tag{6}$$

which from the relation $L(1) = (R_c - 1)^2(2R_c + 1)/2R_c^3$ gives

$$\mathrm{Pe} = \frac{3}{8}\beta_e \frac{(\delta/a)^2(3 + 2\delta/a)}{2(1 + \delta/a)^3}. \tag{7}$$

In the case of full HI ($\delta/a \ll 1$) the motor velocity is small due to the smallness of both β_e and (δ/a),[2] whereas in the opposite limiting case of the absence of HI ($\delta/a \gg 1$) one obtains $\mathrm{Pe} = 3\beta_e/8$ in agreement with Córdova-Figueroa and Brady.[13]

It is worth noting that the latter expression in the absence of HI remains valid for the case of finite ratio r_c/b, *i.e.* finite solute size. One only has to rewrite the dimensionless parameters as: $\mathrm{Pe} = U(r_c + b)/(D_b + D_a)$, $\beta_e = \phi_s(r_c^3/b^2a)(1 + b/r_c)^4(1 + b/a)^{-2} \ll 1$. For, $r_c \gg a$ the above-mentioned redefinitions of Pe and β_e are all that are needed. When HI are included, that is, for $r_c \approx a \geq \delta \approx b$, a full numerical solution is needed; this only results in a quantitative change, however.

For an arbitrary angle α of the active patch an additional factor $1 - \cos^2\alpha$ is the only change to eqn (7), showing that the maximum velocity occurs for a half active motor—a Janus particle.

In terms of a dimensional velocity we have for all HI

$$U = \frac{j_s kT}{8\eta D_b}\delta^2\left(1 + \frac{2}{3}\frac{\delta}{a}\right), \quad \beta_e \ll 1. \tag{8}$$

Note that since $kT/\eta D_b \sim b$ the motor speed is given by the flux per unit area, j_s, times the interactive length squared and the size of the solute: $U \sim j_s\delta^2 b$, which is independent of kT and the solvent viscosity. Note also that the motor speed is set by rate of solute generation compared to that of diffusion, j_s/D_b, which has units of $|\nabla n|$ (number/length^4) and corresponds to the magnitude of the self-generated solute concentration gradient, times the usual diffusiophoretic factor $kT\delta^2/\eta$. Note, however, that eqn (8) is not restricted to small δ/a, but, through the colloidal approach, is shown to apply for all δ/a.

The result eqn (8) agrees with that given by Golestanian *et al.*[12] (with the surface phoretic mobility pointed out by Golestanian[21]). In order to compare the two for the hard-sphere potential of interaction between the motor and solute particles, one has to calculate the Derjaguin length $\lambda_D = \delta/\sqrt{2}$. The work by Golestanian *et al.*[12,21] only considered the limit of small flux rates or small β_e.

2.2 Large flux rates, $\beta_e \gg 1$

In the limit of large β_e, diffusion is small competed to advection and the distribution of the solute product on the reactant part of the surface follows directly from eqn (2b):

$$\hat{n}(r = 1, \mu < 0) = -(\mathrm{Pe}L(1)\mu)^{-1}, \tag{9}$$

and $\hat{n} = 0$ on the chemically passive part. Formally, the concentration field diverges near the boundary between reactive and passive parts $\mu = 0$, and the small diffusivity must be taken into account here (see Appendix A). Fortunately, this detailed analysis is not needed to obtain the velocity of self-propulsion because of the additional factor of μ in eqn (3). Indeed, calculating the integral one arrives at

$$\mathrm{Pe} = \sqrt{\frac{3}{2}\beta_e}. \tag{10}$$

Note that this expression is valid regardless of the level of HI included; the hydrodynamic factor $L(1)$ cancels out of the problem. (Although the limiting value of Pe does not depend on R_c, the asymptotic limit is attained when $\mathrm{Pe}(\delta/a)^3 \gg 1$ for full HI.) Thus, for large flux rates the motor speed can become large, not only because of the large value of β_e, but also because the hydrodynamic hindering factor $(\delta/a)^2$ (coming from $L(1)$, *cf.* eqn (7)) is not present. In dimensional terms we have for all δ/a, *i.e.* all HI

$$U = \sqrt{\frac{3}{2}\frac{D_b{}^2\beta_e}{r_c{}^2}} = \sqrt{2\pi j_s r_c{}^2 D_a} = \sqrt{\frac{j_s akT}{3\eta}}, \quad \beta_e \gg 1 \tag{11}$$

where we have taken $r_c \approx a$ in the last equality as this would be the more common case. In contrast to the case at small flux rates (8), at high flux rates the motor speed is independent of the diffusivity of the products, scales as the square root of the motor size and depends on kT/η.

This result at high flux rates can be understood as follows: The concentration near the reactive site is set by the balance of the advective flux with the rate of production: $nUL(1) \approx j_s$. The resulting osmotic force is thus $kTj_s r_c{}^2/UL(1)$, and for the velocity of self-propulsion one obtains $U \approx j_s r_c{}^2 D_a/U$. Therefore, $U \approx \sqrt{j_s r_c{}^2 D_a}$, in agreement with eqn (11).

The above result differs from that of Jülicher and Prost[14] who predict $U \sim j_s^{2/3}$. Although Jülicher and Prost[14] did not give a formal derivation we believe their result comes from assuming that there is a boundary layer at high Péclet number whose thickness scales as $\mathrm{Pe}^{-1/2}$. Why they may have made this assumption can be understood as follows: There are typically three scalings for concentration/thermal boundary layers at high Pe: $\mathrm{Pe}^{-1/3}$ for a no-slip surface, $\mathrm{Pe}^{-1/2}$ for a slip surface, and Pe^{-1} for flow through a surface (*e.g.* a suction velocity or deposition or a moving front). While it may seem natural to suppose a slip surface, the problem here resembles that of a moving front. The solute flux is zero at the surface $r_c = a + \delta$ (the semipermeable membrane in Fig. 1), but the fluid is allowed to move through this surface coming to zero at the actual motor surface $r = a$. There is a finite advection velocity, and thus advective solute flux, normal to the no-flux surface in eqn (2), namely, the term $\mathrm{Pe}\boldsymbol{e}_z\cdot\boldsymbol{n}L(1)\hat{n}$. If the advective velocity is towards the surface there will be a Pe^{-1} boundary layer in which diffusion and advection balance. However, in this problem the motor motion is away from the reactive portion of the surface and there is no need for a boundary layer; advection balances production on the active surface as discussed above.

2.3 Large flux rates, $\beta_e \gg 1$, arbitrary α

The results at high β_e can be generalized for different reactive patch angles α. We first consider the simplest case of a smaller (than a hemisphere) reactive patch, $\alpha > \pi/2$. In this case the analysis above remains unchanged, but eqn (9) now applies for $\theta > \alpha$ and the integration of the osmotic force results in the additional factor $1 + \cos\alpha < 1$. This factor enters eqn (10) as

$$\mathrm{Pe} = \sqrt{\frac{3}{2}\beta_e(1+\cos\alpha)}, \quad \alpha > \pi/2. \tag{12}$$

A smaller reactive patch obviously reduces the velocity of self-propulsion. This reduction is more pronounced than that for small Pe (where the factor is $1-\cos^2\alpha$) for a nearly spherical patch, $\alpha < \alpha_c = \pi - \arccos[(\sqrt{5}-1)/2] \approx 0.712\pi$. While for even smaller patches, $\alpha > \alpha_c$, although Pe tends to zero in eqn (12) it does so at a slower rate than for small Pe.

The opposite case, $\alpha < \pi/2$, is more complicated and interesting. We first analyze this case for $R_c \gg 1$, no HI. While the solution for $\mu < 0$ is unaffected, for positive μ the behavior is qualitatively different. The motor motion now produces an inflow of solvent (and solute) to the reactive boundary and thus there will be a boundary layer on the upstream portion of the surface, $\mu > 0$, whose thickness scales as Pe^{-1}. The leading order concentration field in the boundary layer is

$$\hat{n}(\mu_0 > \mu > 0) = \frac{\mu(\mu_0-\mu)}{1-\mu^2}\exp(-\rho\mu) + O(\mathrm{Pe}^{-1}), \tag{13}$$

where $\rho = \mathrm{Pe}(r-1)$ is the stretched normal coordinate and $\mu_0 = \cos\alpha$.

On the upstream face of the motor the osmotic force is $O(1)$ and given by

$$\int_0^{\mu_0} \hat{n}(r=1,\mu)\mu\mathrm{d}\mu = \frac{1}{2}\left[\mu_0 \ln\frac{1+\mu_0}{1-\mu_0} + \ln\left(1-\mu_0^2\right) - \mu_0^2\right] \equiv \Psi(\mu_0), \tag{14}$$

in contrast to the $O(\mathrm{Pe}^{-1})$ contribution from the downstream face. Note that $\Psi(\mu_0) \approx \mu_0^4/12$ at small μ_0 and is rather small even for $\mu_0 = 0.5$.

Therefore, combining the two contributions to the osmotic force from the up- and down-stream portions of the motor surface, the self-consistency eqn (3) gives a quadratic equation for the motor speed

$$\mathrm{Pe} = \frac{3\beta_e}{2\mathrm{Pe}}\left[1 - \mathrm{Pe}\,\Psi(\mu_0)\right]. \tag{15}$$

There is an additional contribution from the transition from the downstream to the upstream portions of the motor surface. The structure of this transition zone is detailed in Appendix A where it is shown that eqn (15) becomes

$$\mathrm{Pe} = \frac{3\beta_e}{2\mathrm{Pe}}[1 + \mu_0 I_1 - \mathrm{Pe}\,\Psi(\mu_0)], \tag{16}$$

where the constant $I_1 < 0$ comes from the solution in the transition region and is given by eqn (32).

The quadratic eqn (16) gives

$$\mathrm{Pe} = \frac{3}{4}\beta_e\Psi\left[\sqrt{1 + \frac{8(1+\mu_0 I_1)}{3\beta_e\Psi^2}} - 1\right]. \tag{17}$$

In the limit $\beta_e\Psi^2 \to 0$ corresponding to $\mu_0 \to 0$, eqn (17) reduces to $\mathrm{Pe} \sim \sqrt{\frac{3}{2}\beta_e}$ and we recover eqn (10).

At the other extreme of large $\beta_e\Psi^2$, eqn (17) becomes $\mathrm{Pe} \sim (1 + \mu_0 I_1)/\Psi$, independent of β_e. Once product particles are produced on the upstream proportion of the motor surface, the motor speed no longer increases with product flux, but rather is limited by speed at which the product species diffuse, $U \sim D_b/r_c$. Even a small reactive patch at the upstream surface is able to hinder the motor motion considerably. When the reactive patch is only on the downstream portion of the motor surface the motor can leave behind all the product species and move unhindered into the surrounding fluid. In contrast, when product species are produced on the front of the motor, they hinder the motor's motion as the motor must now push these particles out of its way to move. We shall see this same hindering and limiting behavior in the next section when there are already product particles in solution.

The inclusion of HI into analysis results in replacing Ψ from the downstream potion of the surface in eqn (15)–(17) with $L^2(1)\Psi(\mu_0)/M(1)$, which is typical for HI at large advection.[18] There would also be a numerical modification of the constant I_1 owing to HI.

As a final note, eqn (13) and the resulting motor speed from eqn (17) are technically only valid if there is a boundary layer at high Pe. Since the Péclet number is not large when there is a reactive patch on the upstream surface of the motor, these results are not quantitatively accurate. But the prediction that the motor speed saturates and scales as D_b/r_c is still correct as shown in Fig. 2.

2.4 Finite flux rates, arbitrary β_e, $\alpha = \pi/2$

For finite values of β_e for a Janus motor, $\alpha = \pi/2$, numerical computations were performed; the solution to eqn (2) was found by a finite difference method. Results of calculations are presented in Figs. 2 and 3. It is clear that as β_e increases the dimensionless velocity of the motor increases monotonically and both the asymptotes of small (7) and large (10) Pe agree well with the numerical data. It is also clear that as δ/a decreases, *i.e.* R_c approaches 1, the motor velocity becomes smaller, and eqn (7) works well for a rather large range of β_e, *e.g.* for $\delta/a = 0.1$ the asymptotic formula for small β_e gives satisfactory agreement with the result of computations even for $\beta_e = 10^3$. However, for any fixed δ/a with increase in β_e the motor velocity is determined by eqn (10), which is independent of R_c—one only needs to increase β_e enough.

The product concentration fields are shown in Fig. 3. The increase in the Péclet number (and, hence, in the advective contribution to transport) leads to the development of a concentration 'wake' behind the motor where all the concentration disturbance is localized, in agreement with the

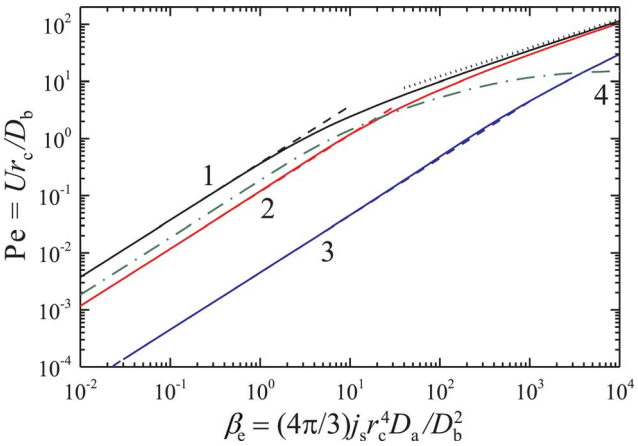

Fig. 2 Variation of the Péclet number with β_e for $R_c = 10^3$ (line 1) $R_c = 2$ (line 2) and $R_c = 1.1$ (line 3). Dashed and dotted lines correspond to the asymptotic results for small β_e, eqn (7), and large β_e, eqn (10), respectively. Line 4 is for a motor that produces products on the upstream surface ($\alpha = 45.6°$, $R_c = 10^3$) showing that the motor speed saturates at high flux rates as predicted in Section 2.3.

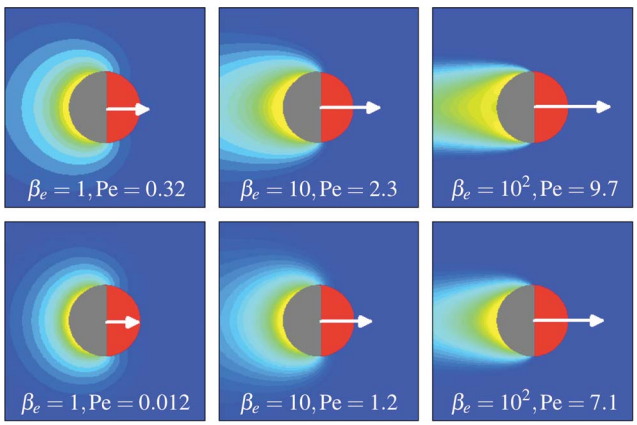

Fig. 3 Concentration fields for a Janus motor for $R_c = 10$ (upper row) and $R_c = 2$ (lower row). The color scales are different for different panels, light corresponds to higher concentration, dark to low concentration ($\hat{n} = 0$).

asymptotic analysis. For smaller values of δ/a (smaller R_c) this effect is less pronounced, since the velocity of the motor (and of the Stokes flow around it) is smaller.

As an example of the speeds attainable by a constant flux motor, for a 1 μm size motor ejecting solute particles that diffuse with a diffusivity corresponding to 1 nm size particles, from eqn (4) $\beta_e \approx 10^6 j_s$, with j_s in units of number/(μm^2 s^{-1}). Thus a flux rate of one reciprocal second per unit area of the motor can result in a large β_e and a motor speed $U \approx 1$ μm s^{-1}.

As shown by Córdova-Figueroa and Brady[13] and Brady[15] the maximum attainable velocity of motor with a surface catalytic reaction, as opposed to a constant flux, is $U \sim D_b/a$, and is independent of concentration of the reactant or fuel. The maximum Péclet number in this case is $O(1)$. Thus a constant flux motor would potentially move faster as its speed continues to increase with flux scaling as $U \sim \sqrt{j_s\, akT/\eta}$. However, the constant flux motor must carry its own fuel, rather than scavenging it from the surrounding fluid as the reactive motor does.

3 Motor motion through a suspension of product species

We now consider the behavior of an osmotic motor immersed in a dispersion of solute particles of radii b at a number density n_∞^p far from the motor. From a colloidal point of view the product particles produced by the motor are thus identical to the solute particles in solution. The reason one needs to consider this problem is that the already existing solute particles will hinder the motion of the motor by enhancing the effective viscosity of the suspending medium. While this hindering will be proportional to the volume fraction of the solute particles, the velocity of the motor is also proportional to the volume fraction (at low to moderate β_e) of the product particles it ejects and thus to be consistent to leading order in concentration, the hindrance of the solute must be considered. We consider the case of a half-active Janus motor, $\alpha = \pi/2$.

The only change needed in eqn (2) is that far away from the osmotic motor we now have a fixed value of the product concentration, $\hat{n}(r \to \infty) = \hat{n}_\infty$, where

$$\hat{n}_\infty = \frac{n_\infty^p}{n_s} = \frac{D_b\, n_\infty^p}{j_s r_c}, \tag{18}$$

which is the ratio of the already existing solute concentration to the characteristic scale for the concentration of flux-generated solute. Setting $\hat{n}_\infty = 0$, one immediately returns to a problem analyzed in Section 2 for the motion of a motor in a free solution.

For a given motor velocity, the boundary value problem for the concentration field is linear and therefore the concentration field can be written as $\hat{n} = \hat{n}_1(\boldsymbol{r}) + \hat{n}_\infty \hat{n}_2(\boldsymbol{r})$, where $\hat{n}_1$ is the solution discussed in Section 2. In determining $\hat{n}_2$ one has to omit the flux of the product particles in eqn (2b) and set $\hat{n}_2 = 1$ at large r. The problem for $\hat{n}_2$ corresponds to the microstructure about a moving 'probe' particle that has been studied in detail in the active microrheology of colloidal dispersions.[17–19]

The unknown motor velocity, and hence the Péclet number, must be found self-consistently. The linearity of the right-hand side of eqn (3) with respect to $\hat{n}$ allows us to write the solution as:

$$\mathrm{Pe} = \frac{3}{2}\frac{\beta_e F(\mathrm{Pe}, R_c)}{1 + \beta\tilde{\eta}(\mathrm{Pe}, R_c)}, \tag{19}$$

where the numerator follows from the problem in Section 2

$$F(\mathrm{Pe}, R_c) = -L(1)\int_{-1}^{1} \hat{n}_1(r = 1, \mu)\mu \mathrm{d}\mu, \tag{20}$$

and denominator is the effective viscosity for the microviscosity problem, $\eta_{\mathrm{eff}}/\eta = 1 + \beta\tilde{\eta}$, with

$$\tilde{\eta} = L(1)\int_{-1}^{1} \hat{n}_2(r = 1, \mu)\mu \mathrm{d}\mu. \tag{21}$$

here, $\beta = \beta_e \hat{n}_\infty$ is the analogue of β_e but based on n_∞^p instead of n_s. The effective viscosity η_{eff}/η was introduced by Squires and Brady[17] for $R_c \gg 1$ (for finite R_c at small and large Pe see Khair

and Brady[19] and Squires[18]).† Although both functions $F(\mathrm{Pe})$ and $\tilde{\eta}(\mathrm{Pe})$ are known, the self-consistency condition (19) must be solved numerically for given β_e and $\hat{n}_\infty$.

Eqn (19) has a simple physical interpretation: while the self-propulsion is created due to asymmetry in the flux-induced part of the concentration field $\hat{n}_1$, the suspension of solute particles itself produces an additional hindrance by increasing the effective viscosity. Thus, the velocity of self-propulsion decreases as $\hat{n}_\infty$ grows.

In the limit of small β_e (or, equivalently, large $\hat{n}_\infty$ at fixed β), when the production of particles is slow enough, the concentration of bath particles is only slightly perturbed from its equilibrium state $\hat{n} = \hat{n}_\infty$. Hence, the Péclet number is also small, and from a regular perturbation expansion it is easy to show that

$$\mathrm{Pe} = \frac{3\beta_e L(1)}{4(2+\beta L(1))}, \quad \beta_e \ll 1. \tag{22}$$

here $\beta_e \ll 1$, whereas β is, in general, finite. This expression agrees with both eqn (7) for $\beta = 0$ and with $\tilde{\eta} = L(1)/2$ at small Pe.[17,18]

Again, similarly to eqn (6) at small β_e the analysis can be extended to the case of finite solute size, r_c/b in the absence of HI, $L(1) = 1$; one only needs to replace the $\hat{n}_\infty$ as follows: $\hat{n}_\infty = n^p_\infty D_b(1 + a/b)/j_s(r_c + b)$, along with the above-mentioned replacements $\mathrm{Pe} = U(r_c + b)/(D_b + D_a)$ and $\beta_e = \phi_s r_c^3/(b^2 a)(1 + b/r_c)^4(1 + b/a)^{-2} \ll 1$.

The opposite limiting case of large β_e can be approached in two different ways. If we increase the rate of production j_s, keeping the concentration of the suspension n^p_∞ fixed ($\beta_e \to \infty$, $\hat{n}_\infty \to 0$, so that β is constant), the matching with eqn (10) takes place. Indeed, in this case the Péclet number is large, *i.e.* $\tilde{\eta} = L^2(1)/4M(1)$.[17] The reaction-induced concentration field $\hat{n}_1$ is given by eqn (9), which results in

$$\mathrm{Pe} = \sqrt{\frac{3\beta_e}{2+\beta L^2(1)/2M(1)}}, \quad \beta_e \gg 1. \tag{23}$$

The situation considered in Section 2 obviously corresponds to $\beta \ll 1$, which ensures the above-mentioned matching with eqn (10).

On the other hand, if both j_s and n^p_∞ grow simultaneously ($\beta \to \infty$ and $\beta_e \to \infty$, so that $\hat{n}_\infty$ is constant), the hindrance to the self-propulsion is mainly caused by the solute bath particles rather than by the solvent. (Technically this requires that $\beta L^2(1)/M(1) \gg 1$, not just $\beta \gg 1$.) Therefore, one can neglect the first term in the denominator in eqn (19) and the self-consistent equation simplifies to

$$\mathrm{Pe} = \frac{3F(\mathrm{Pe})}{2\hat{n}_\infty \tilde{\eta}(\mathrm{Pe})}, \quad \beta_e \gg 1, \beta \gg 1. \tag{24}$$

The value of the Péclet number increases as $\hat{n}_\infty$ decreases, and for $\mathrm{Pe} \gg 1$, $F(\mathrm{Pe}) \sim L(1)/\mathrm{Pe}$ and $\tilde{\eta}(\mathrm{Pe}) = L^2(1)/4M(1)$ giving $\mathrm{Pe} \sim \sqrt{6M(1)/\hat{n}_\infty L(1)}$, which agrees with eqn (23) for large β. Note that in this limit the motor speed saturates at the diffusive velocity of the product particles, $U \sim D_b/r_c$ (times the factor $\sqrt{6M(1)/\hat{n}_\infty L(1)}$).

It should be noted that the limits $\beta_e \gg 1$ and $\hat{n}_\infty \ll 1$ do not commute. In Section 2 the resistance (the inverse mobility of the motor) is determined by the solvent, whereas in eqn (24) the resistance is dominated by the solute. Indeed, for a large motor the contribution of the particles to the resistance grows as r_c^2, whereas solvent drag only grows as a.

For arbitrary values of β_e (and, hence, Pe) numerical solutions for $\hat{n}$ and Pe are found; in the computations we restrict the attention to the particular case of no HI, $R_c \gg 1$, and $L = M = 1$ in order to illustrate most simply the general behavior.

In Fig. 4 we plot the predictions for Pe/β as a function of $\hat{n}_\infty^{-1} = j_s r_c/D_b n^p_\infty$, that is for increasing product flux. The curves correspond to various β and the symbols to Brownian dynamics (BD) simulations[23] (in the simulations we took $r_c = a$ in the definition of the motor self-diffusivity). The agreement is satisfactory, with a discrepancy of a factor of approximately 3/4. The reason for this discrepancy is unclear, but may result from a relatively small r_c/b and relatively large background volume fraction of the solute particles used in the simulations.

The theoretical results agree with the limits of high, eqn (22), and low, eqn (23), $\hat{n}_\infty$. It is clear that Pe/β decays as β increases, although Pe itself grows. It is worth noting that the transition from the limit of high to low $\hat{n}_\infty$ is governed by $\beta_e^{-1} = \hat{n}_\infty/\beta$ rather than by $\hat{n}_\infty$ itself: for smaller β larger values of $\hat{n}_\infty^{-1}$ are needed to agree with asymptotic behavior (23).

In Fig. 5 we plot Pe as a function of β for four different values of $\hat{n}_\infty$ that span the range from small to large. The plot shows that for small β, $\mathrm{Pe} \sim \beta_e = \beta/\hat{n}_\infty$ according to eqn (22). For finite $\hat{n}_\infty$, the motor velocity saturates as $\beta \to \infty$, giving $\mathrm{Pe} \sim O(1)$, which agrees well with eqn (24). The motor moves at a diffusive speed $U \sim D_b/r_c$, with a prefactor decaying as $\hat{n}_\infty^{-1/2}$, showing the effect of additional hindrance caused by the suspended particles. The transition from low to high β regimes occurs near $\beta = 10$. Indeed, to attain the plateau at large β one has only to neglect unity with respect to $\beta\tilde{\eta}$, as seen by comparing eqn (19) and (24).

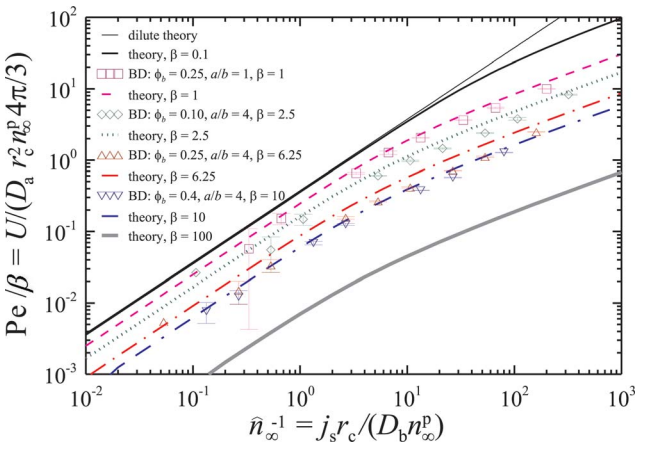

Fig. 4 The ratio $\mathrm{Pe}/\beta = U/(D_a n^p_\infty r_c^2 4\pi/3)$ as a function of $\hat{n}_\infty^{-1} = j_s r_c/D_b n^p_\infty$ for various values of $\beta = (4\pi/3)n^p_\infty r_c^2 b$. The theoretical predictions (lines) are compared to Brownian dynamics simulations (symbols) for same β.[23] (Here HI are neglected, $L = M = 1$, and $r_c = a$.).

† It should be noted that in our analysis the dilute restriction $\eta_{\mathrm{eff}} \approx \eta$ need not be enforced since the Péclet number is not prescribed but is found self-consistently.

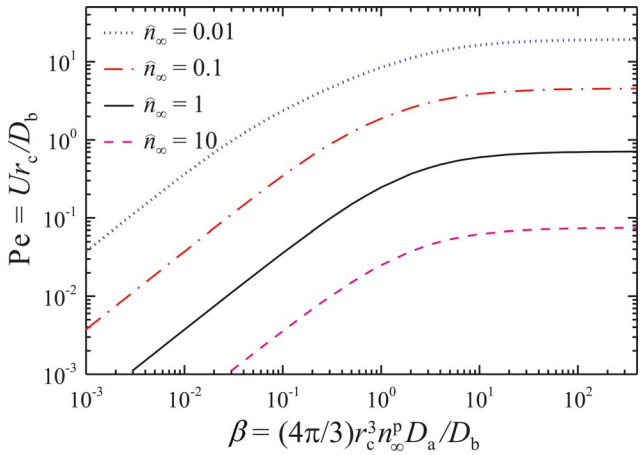

Fig. 5 The Péclet number Pe as a function of β for various $\hat{n}_\infty$. HI have been neglected by setting $M = L = 1$.

Fig. 6 shows density plots around a motor at $\beta = 10$ for different $\hat{n}_\infty$ (top row) and also at $\hat{n}_\infty = 0.1$ for different values of β (bottom row). At large $\hat{n}_\infty$, the flux is small compared to the Brownian motion of the already present product particles and the density is almost symmetric (as it would be at equilibrium). Symmetry breaking is clearly seen for large β, with the presence of a high bath particle density layer on the front of the motor (here $\hat{n}_2$ is dominating) and a high-density comet-like wake behind the motor (the contribution of $\hat{n}_1$, *cf.* Fig. 3). Note that there is no increased concentration in front of the motor in free solution (*cf.* Fig. 3). This wake grows longer as the Péclet number is increased, reflecting the decreasing ability of Brownian motion to heal the disturbed suspension. For these large values of $\beta_e = \beta/\hat{n}_\infty$, one also notes the local concentration of product particles near the equator $\theta = \pi/2$ (see the right column in Fig. 6). This effect can be quantitatively described by eqn (9). It is observed in the density plots that by increasing β and keeping $\hat{n}_\infty$ fixed, the concentration of solute particles is reduced near the reactive surface and increases near the passive. In the high Pe limit, the effect of a moving particle on the suspension is strongly localized to a thin advection-diffusion boundary layer of thickness $O(r_c/\mathrm{Pe})$ on the front of the motor.[17–19]

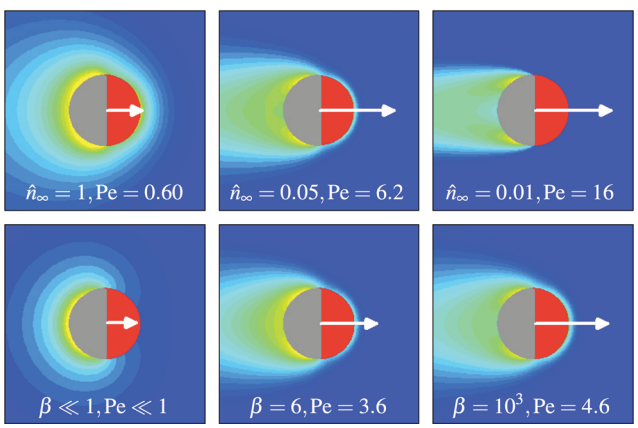

Fig. 6 Solute bath particle density profiles in the symmetry plane of the osmotic motor at $\beta = 10$ for different $\hat{n}_\infty$ (top row) and at $\hat{n}_\infty = 0.1$ for different values of β (bottom row). The colors scales are different for different panels, light corresponds to higher concentration, dark low concentration ($\hat{n} = \hat{n}_\infty$). HI have been neglected by setting $M = L = 1$.

4 Discussion and conclusions

We considered the self-propulsion of an osmotic motor that emits solute particles on a portion of its surface. Both advection of the product species and hydrodynamic interactions between the motor and the solute were taken into account. The limits of slow and fast surface flux were treated analytically, while for arbitrary flux rates numerical simulations were performed. We have also analyzed the motion of the motor through a suspension of solute species whose additional hindrance leads to a decrease in the self-propulsion velocity. Brownian dynamics simulations agreed well with the theoretical predictions.

In contrast to the studies of Golestanian *et al.*,[11,12] we used a colloidal description of the system—both the motor and the product solute were modeled as colloidal particles dispersed in an incompressible solvent. This approach, in general, relaxes the restriction on the motor size, allowing one to consider a motor of size comparable to that of the solute particles. Further, we explicitly considered the effects of advection of the product species, which is essential to consider high flux rates.

We showed that the motion of a motor in a suspension of preexisting product species is hindered by the increased effective viscosity of the suspension, akin to what happens in active microrheology, and this hindrance can lead to a saturation in the motor speed at the diffusive velocity of the products. In the absence of solute in the solution, the motor speed continually increases with the surface flux rate, eventually scaling as the square root of the surface flux.

We also showed, however, that even a small reactive patch on the upstream surface of the motor can drastically change the limiting behavior at high flux rates in the absence of solute in solution, with the motor speed now saturating at the diffusive velocity of the products. These different limiting behaviors suggest that considerable care may be needed when manufacturing motor particles in order to obtain the maximum speeds possible.

Although we have assumed that only a single product species is generated by the motor, the model can be readily extended to polydisperse suspensions of particles and multiple reactant/product species. What is important is the *total* osmotic force acting on the motor, which is given by the sum of the individual osmotic forces created by each species (for dilute systems). The individual forces can be coupled, however, *via* the advective motion of the motor's influence on the concentration distributions. We also assumed that the surface flux was constant in time. As long as the time rate of change of the surface flux is slow compared to the diffusive time scale of the products, the same motor velocity will result using the current value of the flux. Whether or not the generation of product species can be modeled as a simple fixed (or time-dependent) flux from the motor surface may depend on the specific experimental setting. Some situations may be more appropriately modeled as a chemical reaction with a rate that depends on the local value of the concentration.[13]

Appendix

A Matching up- and down-stream concentrations in the transition zone

We briefly discuss the matching of the asymptotic solutions on the up- and down-stream faces for large β_e and $\alpha < \pi/2$. For the sake of simplicity no HI are included, thus $L = M = 1$. The solution on the downstream face is given by

$$\hat{n} = -\frac{1}{\mathrm{Pe}\sqrt{1-r^2(1-\mu^2)}}, r\sqrt{1-\mu^2} < 1, \mu < 0, \quad (25)$$

which provides $\hat{n}(r=1,\mu) = -(\mathrm{Pe}\mu)^{-1}$ at the motor surface, see eqn (9). In order to match this field and the solution valid near the upstream face, eqn (13), and to eliminate the divergence of $\hat{n}(r=1)$ (eqn (25)) at $\mu = 0$ a matching procedure is developed. To that end we introduce stretched coordinates $\xi = (r-1)\mathrm{Pe}^{2/3}$ and $\eta = \mu\mathrm{Pe}^{1/3}$. The concentration field near $\mu = 0$ and $r = 1$ is represented as

$$\hat{n} = \mu_0 \mathrm{Pe}^{-1/3} f_1(\xi,\eta) + \mathrm{Pe}^{-2/3} f_2(\xi,\eta), \quad (26)$$

where both the functions $f_{1,2}$ satisfy the equation

$$\partial_\xi^2 f_j + \eta\partial_\xi f_j + \partial_\eta f_j = 0, (j = 1,2) \quad (27)$$

but with different boundary conditions at $\xi = 0$:

$$\partial_\xi f_1 + \eta f_1 = 0, \partial_\xi f_2 + \eta f_2 = -1, \quad (28)$$

and different asymptotics at $\eta \to +\infty$:

$$f_1 = \left(\eta - \frac{1}{2}\xi^2 + O(\eta^{-1})\right)\mathrm{e}^{-\eta\xi}, \quad (29)$$

$$f_2 = -\left(\eta^2 - \frac{1}{2}\eta\xi^2 + O(\eta^0)\right)\mathrm{e}^{-\eta\xi} \quad (30)$$

and at $\eta \to -\infty$:

$$f_1 \to 0, f_2 \to \frac{1}{\sqrt{\eta^2 - 2\xi}}. \quad (31)$$

It can be easily checked that f_2 provides matching with $\hat{n}$ given by eqn (25), whereas the matching with $\hat{n}$ at positive μ, eqn (13), is ensured by both f_1 (the term proportional to μ_0) and f_2.

Unfortunately, both boundary value problems have to be solved numerically. The contributions of these two fields to the parenthesis in the right-hand side of eqn (15) are given by $\mu_0 I_1$ and $\mathrm{Pe}^{-1/3} I_2$, respectively. Here,

$$I_j = -\int_{-\eta_*}^{\eta_*} \eta \tilde{f}_j(\xi = 0)\mathrm{d}\eta, \quad (32)$$

with $\tilde{f}_1 = f_1 - \eta$ and $\tilde{f}_2 = f_2 + \eta^2$ for $\eta > 0$. (The functions bearing tildes remain finite for $\eta \gg 1$.) The limits of integration $\eta_* = \mu_* \mathrm{Pe}^{1/3}$ are chosen in such a way that $\mu_* \ll 1$, whereas $\eta_* \gg 1$.

One can see that I_1 is of order unity and hence it must be taken into account in eqn (15) as was done in writing eqn (16). Moreover, numerically Pe may not be very large, and therefore the $O(\mathrm{Pe}^{-1/3})$ contribution of I_2 also plays an important quantitative role. Note that this term remains even for $\mu_0 = 0$.

References

1 S. Sengupta, M. E. Ibele and A. Sen, *Angew. Chem., Int. Ed.*, 2012, **51**, 8434–8445.
2 G. A. Ozin, I. Manners, S. Fournier-Bidoz and A. Arsenault, *Adv. Mater.*, 2005, **17**, 3011–3018.
3 R. W. Obrien and L. R. White, *J. Chem. Soc., Faraday Trans. 2*, 1978, **74**, 1607–1626.
4 I. Goldhirsch and D. Ronis, *Phys. Rev. A*, 1983, **27**, 1616–1634.
5 J. L. Anderson, *Annu. Rev. Fluid Mech.*, 1989, **21**, 61–99.
6 R. W. Applegate, J. Squier, T. Vestad, J. Oakey and D. W. M. Marr, *Opt. Express*, 2004, **12**, 4390–4398.
7 W. F. Paxton, S. Sundararajan, T. E. Mallouk and A. Sen, *Angew. Chem., Int. Ed.*, 2006, **45**, 5420–5429.
8 J. R. Howse, R. A. L. Jones, A. J. Ryan, T. Gough, R. Vafabakhsh and R. Golestanian, *Phys. Rev. Lett.*, 2007, **99**, 048102.
9 H.-R. Jiang, N. Yoshinaga and M. Sano, *Phys. Rev. Lett.*, 2010, **105**, 268302.
10 P. A. Giardini, D. A. Fletcher and J. A. Theriot, *Proc. Natl. Acad. Sci. U. S. A.*, 2003, **100**, 6493–6498.
11 R. Golestanian, T. B. Liverpool and A. Ajdari, *Phys. Rev. Lett.*, 2005, **94**, 220801.
12 R. Golestanian, T. B. Liverpool and A. Ajdari, *New J. Phys.*, 2007, **9**, 126.
13 U. M. Córdova-Figueroa and J. F. Brady, *Phys. Rev. Lett.*, 2008, **100**, 158303.
14 F. Jülicher and J. Prost, *Eur. Phys. J. E: Soft Matter Biol. Phys.*, 2009, **29**, 27–36.
15 J. F. Brady, *J. Fluid Mech.*, 2011, **667**, 216–259.
16 N. Sharifi-Mood, J. Kpolik and C. Maldarelli, *Phys. Fluids*, 2013, **25**, 012001.
17 T. M. Squires and J. F. Brady, *Phys. Fluids*, 2005, **17**, 073101.
18 T. M. Squires, *Langmuir*, 2008, **24**, 1147–1159.
19 A. S. Khair and J. F. Brady, *J. Fluid Mech.*, 2006, **557**, 73–117.
20 W. B. Russel, D. A. Saville and W. R. Schowalter, *Colloidal Dispersions*, Cambridge University Press, 1992.
21 R. Golestanian, *Phys. Rev. Lett.*, 2009, **102**, 188305.
22 J. Happel and H. Brenner, *Low Reynolds Number Hydrodynamics*, Prentice-Hall, 1965.
23 U. M. Córdova-Figueroa, PhD thesis, California Institute of Technology, 2008.